TISSUE ENGINEERING: Part C
Volume 19, Number 12, 2013

DOI: 10.1089/ten.tec.2012.0712

A Novel Native Derived Coronary Artery Tissue-Flap Model

Hug Aubin, MD,[1] Alexander Kranz, (cand. med.),[1] Jörn Hülsmann, MSc,[1]
Antonio Pinto, PhD,[1] Mareike Barth, PhD,[1,2] Andrey Fomin, MSc,[1]
Artur Lichtenberg, MD,[1] and Payam Akhyari, MD[1]

Although tissue-engineering approaches have led to significant progress in the quest of finding a viable substitute for dysfunctional myocardium, the vascularization of such bioartificial constructs still remains a major challenge. Hence, there is a need for model systems that allow us to study and better understand cardiac and vascular biology to overcome current limitations. Therefore, in this study, *in toto* decellularized rat hearts with a patent vessel system were processed into standardized coronary artery tissue flaps adherent to the ascending aorta. Protein diffusivity analysis and blood perfusion of the coronary arteries showed proper sealing of the de-endothelialized vessels. Retrograde aortic perfusion allowed for selective seeding of the coronary artery system, while surface seeding of the tissue flaps allowed for additional controlled coculture with cardiac cells. The coronary artery tissue-flap model offers a patent and perfusable coronary vascular architecture with a preserved cardiac extracellular matrix, therefore mimicking nature's input to the highest possible degree. This offers the possibility to study re-endothelialization and endothelial function of different donor cell types and their interaction with cardiac cells in a standardized biologically derived cardiac *in vitro* model, while establishing a platform that could be used for *in vitro* drug testing and stem cell differentiation studies.

Introduction

Rising epidemiologic numbers of cardiovascular disease and the current demographic trend turn heart disease into an increasing health economic problem worldwide, with coronary artery disease being one of the leading causes of mortality in the western world.[1] In the recent years, the emerging field of cardiovascular tissue engineering has developed new experimental strategies in the treatment of heart disease. Different approaches are currently pursued to generate functional heart tissue to regenerate, restore, or replace the injured myocardium.[2] However, one of the key limitations in all tissue-engineering approaches—the vascularization of engineered functional tissues—still remains a major challenge.[3]

Nearly all native tissues regulate oxygen and nutrient supply as well as carbon dioxide and waste removal *in vivo* through a complex, ramified system of blood vessels that are subsequently divided into smaller subunits until forming a system of small capillaries with a maximal distance between capillaries of less than 200 μm[4] correlating with the diffusion limit of oxygen.[5] Additionally, a functional network of endothelial cells (EC) coating the blood vessels, the so-called endothelium, is needed to prevent thrombogenicity, to act as a selective permeable barrier ensuring active and passive molecule transport, to regulate blood pressure, and to enhance angiogenesis into the circumjacent tissue among many other complex physiological functions.[6] Therefore, functional vascularization—defined as an intact endothelial layer covering the inner surface of ramified vessel structures with a maximal distance between each other of approximately 200 μm—seems to be a prerequisite for engineered tissues to be viable *in vivo*.

Vascularization strategies are still a question of intensive debate in the tissue-engineering community.[3] Approaches range from trying to induce angiogenesis and vasculogenesis *in vivo* using biological stimuli to prevascularization strategies using synthetic or *native derived* scaffolds with preformed vascular systems *in vitro*. Cell populations for *in vitro* models of angiogenesis and vasculogenesis vary from human dermal microvascular ECs (HDMECs) to human umbilical vein ECs (HUVECs) and endothelial progenitor cells (EPCs) among others, with additional coculture modalities involving nonendothelial cells that may further support and partially enhance angiogenic mechanisms.

However, the vascular system of the heart is an integrated system of particular complexity, consisting of several endothelial compartments, including ECs of coronary arteries, capillaries, and endocardium, each differing in developmental origin, structure, and function.[7] The native coronary artery system originates from the ascending aorta with the ostia of the left and right coronary artery (LCA and RCA,

[1]Department of Cardiovascular Surgery, Heinrich-Heine-University Düsseldorf, Düsseldorf, Germany.
[2]Institute for Pharmacology and Clinical Pharmacology, Heinrich-Heine-University Düsseldorf, Düsseldorf, Germany.

respectively), located in the sinuses of the aortic valve. LCA and RCA ramify into epicardial arteries, which give rise to smaller intramural arteries penetrating the myocardium and subsequently branching into arterioles, which narrow into a capillary network surrounding the adjacent cardiomyocytes. The number of myocardial ECs outnumbers the number of cardiomyocytes by a ratio of approximately 3 to 1, with the distance between a capillary EC and the nearest cardiomyocyte reaching only 1 μm and, thus, providing optimal diffusion of oxygen and nutrients between the blood and underlying myocardium.[8] This unique architecture of the coronary vascular system, allowing for intimate contact and reciprocal interaction between the endothelium and cardiomyocytes, is critical for the physiological function of the heart. Hence, there is a need for standardized models recapitulating the cardiac endothelial microenvironment *in vitro* that will allow us to study and better understand the cardiac and vascular biology to overcome current limitations.

In the past—following the *in toto* heart decellularization concept introduced in 2008[9]—we developed a system for the high volume generation of reproducible acellular heart scaffolds through automated software-controlled coronary perfusion that not only preserves the basic anatomy of the heart as well as the basic extracellular matrix (ECM) characteristics, but also conserve the geometry and patency of the native coronary vascular system.[10] In this study, we used those acellular heart scaffolds to create a standardized *native derived* coronary artery tissue-flap model to study re-endothelialization and endothelial function of tissue-engineered cardiac constructs, while establishing a platform that could be used for *in vitro* drug testing and stem cell differentiation studies.

Materials and Methods

All animal experiments and surgical procedures were performed in compliance with the Guide for the Care and Use of Laboratory Animals as published by the US National Institutes of Health (NIH Publication 85-23, revised 1996) and were approved by the local animal care committees (registr. nr. A/224/2009).

Whole heart decellularization

Hearts of Wistar rats (female and male, 350 to 450 g) were explanted and decellularized *in toto* by standardized coronary perfusion through automated software-controlled retrograde aortic perfusion as previously described.[11] For chemical decellularization, we used a simplified decellularization protocol that we have successfully used for the decellularization of heart valves in the past. Briefly, it consists of perfusion with 0.5% sodium dodecyl sulfate (SDS; Carl-Roth) and 0.5% desoxycholic acid (DCA; Amresco) for 48 h with subsequent perfusion with deionized water and phosphate-buffered saline (PBS; Gibco) for 24 and 72 h, respectively. Decellularized hearts were stored in PBS supplemented with penicillin/streptomycin at 4°C before further processing.

Integrity and patency of the coronary vascular system

For the demonstration of the integrity and patency of the coronary vascular system after the decellularization process, whole hearts were perfused with epoxide resin (E20; Biodur) and desiccated afterward. High-resolution macroscopic pictures of the LCA and RCA system were taken with an EOS 400d (Canon) camera and perfused vessels up to 4th order ramifications were counted manually.

Standardized native derived coronary artery tissue-flap model

The standardized coronary artery tissue-flap model was created by microsurgical dissection of the decellularized whole hearts into two tissue flaps adherent to the ascending aorta and encasing the LCA and RCA, respectively. The transluminescence of the decellularized tissue flaps allowed for live imaging via a common inverse field microscope (DM IL LED; Leica) or confocal microscope (LSM 700; Zeiss). Selective catheterization of the coronary ostia via a 28G catheter (Braun) allowed for standardized perfusion of the tissue flaps via the respective de-endothelialized or repopulated main coronary arteries and subsequent vessel system with no perfusate loss, either manually with a syringe or with a syringe pump ensuring a constant flow rate.

Coronary artery tissue-flap models with an *in vitro* repopulated vessel system were created in a two-step procedure. In the first step, the coronary artery vessel system of the whole hearts was cell seeded through coronary perfusion via retrograde aortic perfusion with a cell density of 5×10^5 cells mL^{-1} and incubated in the cell-specific standard culture medium in a standard cell culture incubator (Forma Scientific) at 5% CO_2 atmosphere and 37°C. After 24 h, in a second step, repopulated whole hearts were dissected into the above-described coronary artery tissue-flap model under sterile conditions and further incubated for 5 days with a medium renewal via manual coronary perfusion every 12 h. For controlled coculture with primary cardiac cells, coronary artery tissue flaps were surface seeded with cells at a density of 2×10^5 cells mL^{-1} immediately after dissection and cultivated for at least an additional 24 h.

Protein diffusivity

For evaluation of the protein diffusion properties, coronary ostia of cell-free coronary artery tissue flaps were selectively catheterized and perfused with a protein solution consisting of 0.0025% Alexa Fluor 555-conjugated albumin bovine serum (fluorescent conjugated BSA; Invitrogen) and 0.1% native bovine albumin serum (BSA; Sigma-Aldrich) dissolved in PBS. Perfusion was carried out via direct coronary perfusion at a rate of 0.1 mL min^{-1} using a common syringe pump (Braun). To quantify diffusion from the main vessels into the circumjacent tissue, fluorescence intensity (FI) was calculated from fluorescent images taken at repetitive time points for a total duration of 60 min with standardized optical capture parameters using an inverse field microscope (DM IL LED; Leica). Therefore, FI was measured and processed at fixed distances from the targeted main vessel wall (up to 550 μm) and averaged for standardized regions of 0,03 mm^2 in both directions from the vessel plane using built-in features of ImageJ (ImageJ, NIH) adjusting for the background intensity caused by matrix fluorescence. FI, assumed to be proportional to the concentration of the fluorescent-conjugated BSA, was then normalized to the midvessel intensities of each sample to account for increasing intensities in progressive images caused by diffusion into the circumjacent tissue along the floor and ceiling of the vessel.

Blood perfusion

Acellular and repopulated coronary artery tissue flaps were selectively catheterized with a 28G catheter as described above and the coronary artery vessel system was perfused with fresh human whole blood, drawn from a peripheral vein and citrated to ensure anticoagulation, for evaluation of vessel patency and sealing for cellular blood components.

Cell studies

For cell studies, we used a standard murine fibroblast cell line (3T3 cells; NIH) to assess the selective *in vitro* coronary artery repopularization capacity and suitability of the presented coronary artery tissue-flap model. 3T3 cells were maintained in the Dulbecco's modified Eagle's medium (DMEM; Gibco) supplemented with 10% fetal bovine serum (FBS) and 1% penicillin/streptomycin (P/S) and were passaged twice per week.

Cell viability was analyzed by live/dead assay assessing the intracellular esterase activity and plasma/nuclear membrane integrity, incubating repopulated coronary artery tissue flaps with calcein-AM and ethidiumhomodimer (Invitrogen) or SYBR-Green I (Invitrogen) and propidiumiodide (PI; Invitrogen), following the manufacturer's instructions. Vital cells fluoresced green either due to the intracellular esterase activity hydrolyzing the calcein-AM substrate to a green fluorescent product or because of active SYBR-Green transport inside the cell nuclei, while nonvital cells fluoresced red due to the membrane permeability and nucleic acid affinity of the red fluorescent ethidiumhomodimer and PI.

For proving the concept of a functional coronary artery tissue-flap model, tissue flaps were re-endothelialized with HUVECs and subsequently surface seeded with primary isolated cardiac cells from neonatal rat hearts. HUVECs were maintained in the endothelial cell basal medium (ECBM MV; PromoCell) with recommended supplements (ECBM MV Supplement Pack; PromoCell), passaged at reaching 60–70% confluence and used at passage 5 for re-endothelialization studies. Before seeding, HUVEC suspension was labeled with green fluorescent 5-chlorormethylfluorescein diacetate (CMFDA, CellTracker™ Green; Invitrogen) for live cell tracking according to the manufacturer's protocol. CMFDA passively diffuses into cells and is cleaved by intracellular esterases to yield a highly fluorescent cell-impermeable substrate that reacts with thiols, forming fluorescent conjugates that are retained inside the cell. Cardiac cells were isolated from neonatal rat hearts as previously described[12] and were maintained in the standard culture medium (M-199; Gibco) supplemented with 10% horse serum, 2% fetal bovine serum, and 1% penicillin/streptomycin (P/S). For coculture experiments, cell suspensions of first passage primary cardiac cells (containing cardiomyocytes as well as cardiac fibroblasts) were labeled with red fluorescent CMTPX (CellTracker™ Red; Invitrogen) for live cell tracking according to the manufacturer's protocol, analogically to the CMFDA labeling, and cardiac cells were then surface seeded on the re-endothelialized coronary artery tissue flaps as described above.

All cells were cultured in a standard cell culture incubator (Forma Scientific) at 5% CO_2 atmosphere and at 37°C. Images were captured using an inverse field microscope (DM IL LED; Leica) or a confocal microscope (LSM 700; Zeiss).

Histology

For histological analysis, cell-free and repopulated coronary artery tissue flaps were fixed in a 4% buffered formaldehyde solution (Roth) and processed via cryostat sectioning (CM 1950; Leica) using standard protocols. Frozen sections of 6 μm were then stained with hematoxylin and eosin (H&E) and Movat's pentachrom staining according to standard protocols as well as with DAPI and phalloidin (Alexa Fluor 555; Invitrogen) for nuclear and cytoskeletal staining according to the manufacturer's protocol, and then visualized using a transmission light microscope (DM 2000; Leica).

Results

Coronary artery vessel system after in toto heart decellularization

Rat hearts were decellularized *in toto* (Fig. 1A) by standardized coronary perfusion through automated software-controlled retrograde aortic perfusion as previously described[10] using a simplified decellularization protocol that we have successfully used for the decellularization of heart valves in the past.[11] All decellularized hearts showed intact heart geometry with complete removal of cellular components and a high degree of critical ECM and basement membrane protein conservation as already previously published.[10] Further, macro- and microscopical analysis of the coronary vascular system after the decellularization process showed complete removal of donor ECs along an intact vascular bed with open lumina and free of decellularization remnants, such as cellular detritus (Fig. 1C, D), revealing an intact acellular vessel system. Retrograde aortic perfusion of the *in toto* decellularized hearts with epoxide resin and subsequent desiccation for visualization, demonstrated uniform perfusion through the complete coronary artery tree down to the capillary system indicating the patency and integrity of the ECM skeleton of the coronary artery vessel system despite coronary perfusion-based decellularization (Fig. 1B and Supplementary Movie SM1; Supplementary Data are available online at www.liebertpub.com/tec). Additionally, perfused vessels up to the ramifications of 4th order were counted individually for the respective left and right coronary system for a total of 4 *in toto* decellularized hearts, averaging 47 ± 19 perfused 4th order branches for the left and 21 ± 11 for the right coronary system (Supplementary Fig. S1).

Standardized coronary artery tissue-flap model

Taking advantage of the intact and patent ECM skeleton of the coronary arteries, we used the *in toto* decellularized hearts to create a *native derived* coronary artery tissue-flap model. Therefore, the left and the right ventricles of the decellularized hearts were each dissected into two quadratic tissue flaps of ca. 0.5 to 1 cm^2 framing the main branches of the LCA and the RCA, respectively, while preserving adherence to the aortic bulbus (Fig. 2A). Thereby, we gained two acellular tissue flaps of defined size and ECM characteristics directly derived from the native heart tissue and each perfused by a main vessel and its branches directly derived from the two main coronary arteries (Fig. 2B, C).

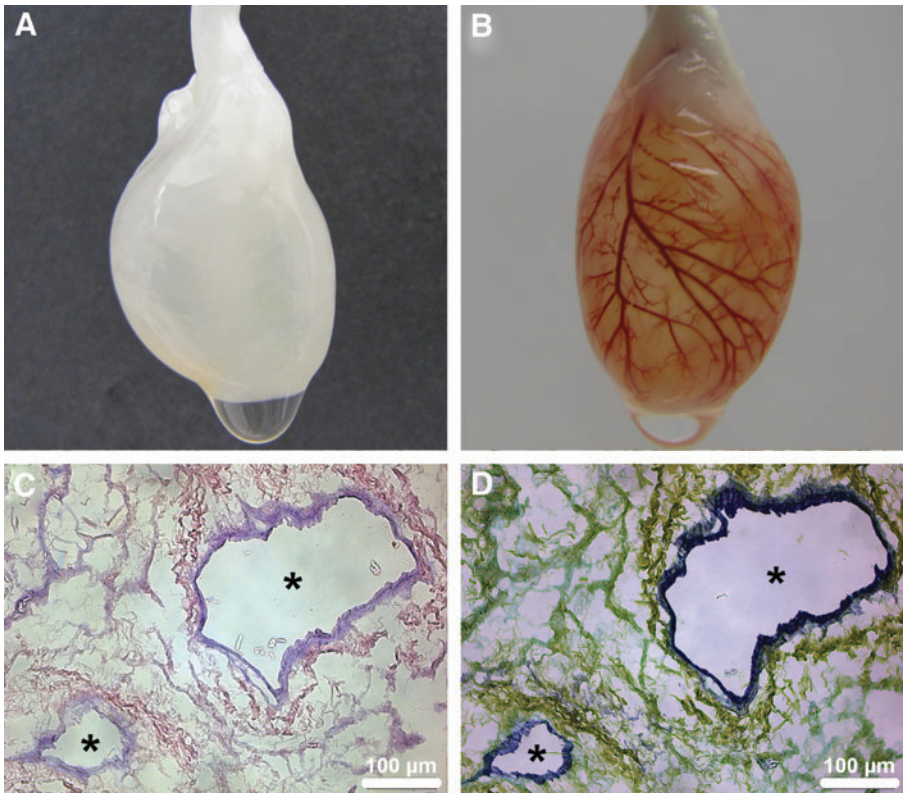

FIG. 1. Coronary artery vessel system after *in toto* heart decellularization. The extracellular matrix (ECM) skeleton of the coronary artery vessel system of the *in toto* decellularized hearts remains intact and patent despite coronary perfusion-based decellularization. **(A)** Representative macroscopic image of an *in toto* decellularized rat heart through automated software-controlled coronary perfusion. **(B)** Retrograde aortic perfusion with epoxide resin and subsequent desiccation of an *in toto* decellularized rat heart shows a patent and intact coronary artery vessel system with uniform perfusion reaching into the capillary system. **(C)** and **(D)** represent H&E and Movat staining, respectively, of an *in toto* decellularized heart showing endothelium-free vessels (*) with open lumina and intact vascular bed. Color images available online at www.liebertpub.com/tec

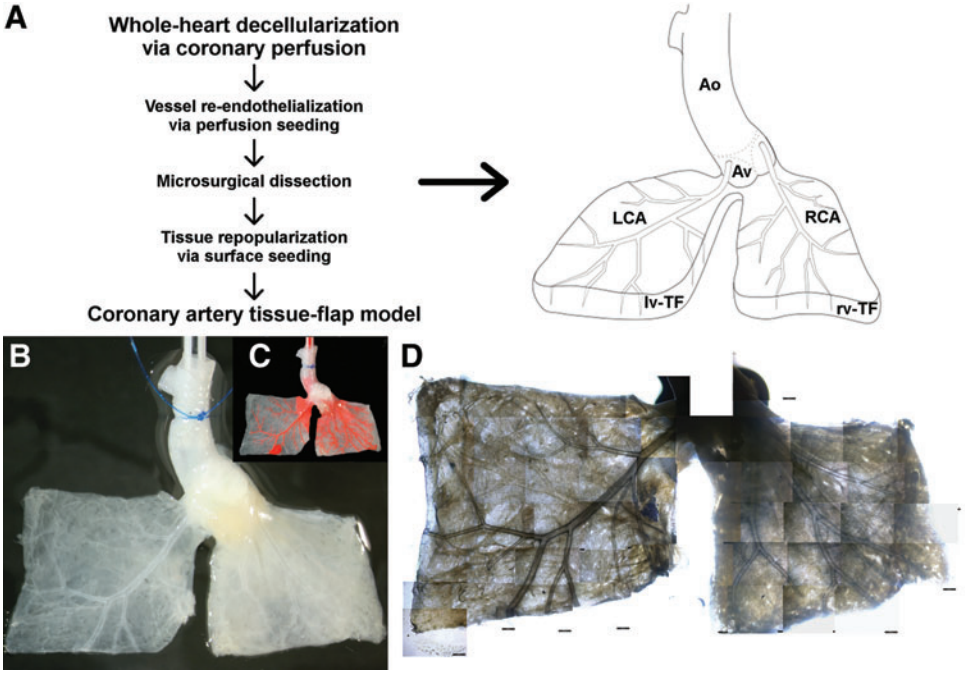

FIG. 2. Standardized *native derived* coronary artery tissue-flap model. Out of an *in toto* decellularized heart, we created a standardized coronary artery tissue-flap model consisting of two defined rectangular acellular tissue flaps originating from the left and right ventricle that, respectively, encase the main branches of the de-endothelialized LCA and RCA, while maintaining adherence to the aortic bulbus. **(A)** Workflow and schematics of the coronary artery tissue-flap model. Ao, aorta; Av, aortic valve; LCA, left coronary artery; RCA, right coronary artery; lv-TF, left-ventricular tissue, flap; rv-TF, right-ventricular tissue flap. **(B)** Representative macroscopic image of a coronary artery tissue-flap model showing the de-endothelialized vessel system of the LCA and RCA, respectively. **(C)** Same model perfused with epoxid resin for better visualization of the coronary artery vessel system. **(D)** Collage of bright field images taken with a common inverse light microscope of the same model at 4×magnification illustrating the potential for live imaging. Color images available online at www.liebertpub.com/tec

Patency and integrity of the coronary artery vessel system of the respective left- and right-ventricular flap was evaluated by epoxide resin perfusion through retrograde aortic perfusion, revealing an intact vascular system as already seen in the perfused whole hearts ($n=4$, data not shown). The transluminescence of the decellularized matrix allowed for live imaging of the respective coronary artery tree through bright field imaging using a common inverse field or confocal microscope (Fig. 2D). Additionally, the reduced thickness of the ventricular walls after decellularization allowed not only imaging and analysis of the main epicardial vessels, but also of the deeper laying endomyocardial branches of the RCA as well as of the LCA despite the thicker ventricular wall of the left ventricle.

Protein diffusivity and blood perfusion of the de-endothelialized coronary artery vessel system

The properties of the de-endothelialized coronary artery vessel system were assessed in terms of passive protein diffusivity through the vessel ECM skeleton into the circumjacent tissue and whole blood perfusibility through the vessel system. To visualize the diffusion of proteins through the de-endothelialized vessels into the circumjacent tissue, fluorescent-conjugated BSA (66 kDa) was perfused at a constant flow rate of 0.1 mL min^{-1} into the coronary artery tissue-flap model via direct coronary perfusion through selective coronary ostia catheterization, while fluorescence images of comparable vessels (in dimensions and ramification patterns) and surrounding tissue were taken at repetitive time points. Sharply defined vessel boundaries immediately after perfusion start and, until perfusion, end without gross perfusate leaks into the circumjacent tissue indicated proper sealing and retained integrity of the coronary artery ECM skeleton despite complete de-endothelialization through the decellularization process (Fig. 3A, B). FI—which is expected to be proportional to the tissue concentration of fluorescence-conjugated BSA—was further analyzed for standardized regions of 0.03 mm^2 in up to 550 μm distance from the targeted vessels. Quantitative analysis of averaged FI showed steadily increasing protein diffusion into the circumjacent tissue as a function of time and distance from the main vessel (Fig. 3C, D). The protein concentration in the tissue circumjacent to the targeted vessel increased over time, while decreasing with incremental distance, however, reaching saturation after ca. 30 min of perfusion at 150 μm distance, with FI normalized to the midvessel intensity of 0.82 ± 0.04, and after ca. 50 min at 550 μm distance, with FI of 0.81 ± 0.29 ($n=4$). Representative diffusion patterns at 150-, 350-, and 550-μm vessel distance and 10-, 20-, and 50-min perfusion time are shown in Fig. 3C and D ($n=4$). However, despite in-sample homogeneity, intersample diffusion patterns obtained by quantitative analysis of FI varied highly depending on the analyzed sample and the targeted vessel because of anatomic variances in tissue vascularization and matrix inhomogeneity caused by the decellularization process, as is indicated by the relatively high standard deviations in Fig. 3C and D.

Directed coronary perfusion with citrated whole blood through selective coronary ostia catheterization of the acellular tissue flaps showed retained patency for cellular blood components with no gross erythrocyte extravasation into the circumjacent tissue of the main and dependent vessels (Fig. 3E–G and Supplementary Movie SM2). Competent drainage of the blood components downstream along the greater vessel openings at the edge of the tissue flaps as well as into the capillary system could be observed. In isolated spots, erythrocytes accumulated and leaked through the capillary system (Fig. 3E). Blood perfusion studies demonstrated full blood compatibility in terms of vessel patency and integrity ($n=3$).

Selective coronary artery repopularization

The selective repopularization capacity and suitability of the de-endothelialized coronary artery vessel system was assessed using a murine fibroblast cell line (3T3 cells) because of its high-proliferation capacity and adherence properties. Therefore, the *in toto* decellularized hearts were perfused with a 3T3 cell suspension of 5×10^5 cells mL^{-1} through retrograde aortic perfusion and cultivated for 24 h allowing for cell adherence to the vessel ECM in a first step. Subsequently, the perfusion-seeded hearts were dissected into the above-described coronary artery tissue-flap model and cultivated for additional 5 days with medium renewal through manual coronary perfusion every 12 h allowing for cell proliferation and migration along the coronary artery vessel system in a second step.

To determine the seeding efficacy through coronary artery cell perfusion, remaining cells in the perfusate after coronary artery perfusion as well as the cells in the medium and bottom of the six-well plates, in which, the hearts were cultivated for the first 4 h, were counted. By subtracting those cells from the initial amount of cells seeded, we could determine that $92.7\% \pm 10\%$ of cells were successfully retained inside the vessel system of the tissue flap ($n=3$).

Following cultivation, live/dead assay with calcein-AM and ethidiumhomodimer as well as with SYBR-Green and PI demonstrated almost exclusive vital cells throughout the RCA and LCA vessel tree inside the respective right and left ventricular flaps ($n=3$) (Fig. 4A–H). Vital cells showed elongated cell morphology of their cell bodies as well as of their cell nuclei with cells consistently colonizing not only larger main vessels of up to 250 μm of diameter (Fig. 4E), but also extending themselves into the capillary system deep inside the myocardial matrix forming single strands of cell nuclei along capillary-like structures (Fig. 4H), as was demonstrated by 3D confocal microscope imaging. The cells inside the coronary vessel system extended themselves consistently throughout the complete perimeter of the vessel system of the tissue flaps, starting at the main coronary arteries and extending themselves to the edge of the tissue flaps (Fig. 4D). Further histological analysis via DAPI, H&E, and Movat staining, revealed tissue repopularization to be highly selective to the vessel system, with apparent cell adherence to the vessel ECM skeleton, as cells remained inside the vessel perimeters with no visible gap to the inner vessel surface despite intermittent vessel perfusion during tissue-flap cultivation and without cell migration into the adjacent myocardial tissue (Fig. 5A–F). In addition to cells clearly lying inside the vessel system, cell clusters that initially seemed randomly distributed inside the tissue matrix were subjected to a more detailed analysis by serial evaluation of neighboring histological sections that demonstrated those clusters to lie within structures pertaining to the coronary capillary system. Additionally, cross sections of repopulated

coronary artery tissue flaps indicated that vessel lumina remained patent after repopularization. In the histological slides, cell-free lumina could be consistently identified and lumen diameters measured to range from ca. 100 μm down to ca. 10 μm, despite being populated with morphologically elongated cells confluently coating the luminal vessel side of the coronary artery system, as was demonstrated by cytoskeletal and nuclear labeling via phalloidin/DAPI staining in repetitive histological slides (Fig. 5G–I).

Blood perfusion

To confirm the patency of the repopulated vessel system, repopulated right-ventricular flaps (3T3, 5×10^5 cells mL^{-1}), as described above, were selectively catheterized and perfused with citrated whole blood, after 5 days of culture and subsequent staining with SYBR-Green/PI to confirm successful repopularization with vital cells. In all repopulated tissue flaps, the catheterized part of the coronary artery system was still patent, even partially filling the remaining capillaries with blood ($n=3$) (Fig. 6A). Microscopic live imaging during blood perfusion revealed repopulated vessels to be patent and to ensure perfusibility of cellular blood components, such as erythrocytes, even down to capillary-like structures (Fig. 6B–E and Supplementary Movie SM3).

Proof of concept

After evaluating the selective vessel repopularization capacity, the concept of a functional coronary artery tissue-flap model was proved by re-endothelialization of the left- and right-ventricular tissue flaps with HUVECs and additional coculture with primary isolated cardiac cells from neonatal rat hearts, as described above. Before seeding, HUVEC suspension was labeled with green fluorescent CMFDA for live cell tracking. Live fluorescent imaging of the myocardial tissue 24 h after HUVEC seeding via coronary perfusion (5×10^5 cells mL^{-1}) showed that extensive endothelial networks had formed inside the perimeters of the coronary vessel system of the decellularized scaffolds (Fig. 7A). Confocal imaging of repopulated tissue flaps revealed consistent 3D vascular structures of varying sizes down to capillary-like structures throughout all the tissue flaps (Fig. 7B, C and Supplementary Movie SM4) ($n=4$). Subsequent surface seeding (2×10^5 cells mL^{-1}) of the re-endothelialized coronary artery tissue flaps with prior red fluorescent CMTPX-labeled primary cardiac cells and additional cultivation for 24 h led to cardiac cells in direct juxtaposition to endothelialized vessels as demonstrated by live confocal imaging (Fig. 7D, E) ($n=3$). Therefore, additional surface seeding led to a successful coculture in all the respective left- and right-ventricular flaps. However, after 24 h of cultivation, the cardiac cell distribution and density was not homogenous throughout the tissue flaps, with cardiac cells mainly concentrating on the surface and with only partial tissue penetration (Supplementary Fig. S2), indicating the need for improving seeding and culture conditions.

Discussion

Despite great progress in the engineering of bioartificial tissues, commercially and/or clinically relevant tissue-engineering applications, such as functional *in vitro* test systems and viable *in vivo* transplants, have yet to become reality in most cases. This entails that regenerative medicine approaches still lag behind their potential promises and most industrial tests concerning pharmaceutical drug and biocompatibility scopes are still traditionally performed using cell monolayers *in vitro* or animal models *in vivo*. One of the main reasons for this lack of success lies in one of the key limitations in tissue engineering, the vascularization of engineered functional tissues.[3] Current vascularization strategies are usually cell or scaffold based with their respective assets and drawbacks, such as the potential for neoangiogenesis versus the need for prevascularization of purely cell-driven approaches, over the high biocompatibility versus the difficult standardization of biological scaffolds, to the high-volume production versus the need for biofunctionalization of synthetic materials. Therefore, there is a need for new vascularized models that will allow us to further study and recreate vascular biology, while helping to evaluate vascularization strategies of engineered functional tissues.

In this study, we present a novel *native derived* coronary artery tissue-flap model, which is a vascularized tissue model originating from native cardiac tissue. This

FIG. 3. Protein diffusivity and blood perfusion through the de-endothelialized coronary artery vessel system. Protein diffusion was assessed via selective catheterization of the coronary ostia and coronary perfusion with Alexa Fluor 555-conjugated BSA (66 kDa) at a constant flow rate of 0.1 mL min^{-1}, while fluorescence images of representative targeted vessels and surrounding tissue were taken at defined time points. Analysis of protein concentrations—proportional to the fluorescence intensity (FI)—showed steadily increasing protein diffusion into the circumjacent tissue as a function of time and distance to the targeted vessel, with no gross perfusate leaks and sharply defined vessel borders indicating proper vessel sealing. Additionally, perfusion with citrated whole blood of selectively catheterized tissue flaps showed patency for cellular blood components with no erythrocyte extravasation of main and dependent vessels into the circumjacent tissue and drainage of the blood components down to the capillary system and along the greater vessel openings at the edge of the tissue flaps. **(A)** Representative bright field as well as fluorescent images of targeted coronary vessel and circumjacent tissue at 1 and 45 min of coronary perfusion with fluorescent-conjugated BSA (red), respectively. White rectangle, region of interest (ROI) for protein diffusivity analysis. **(B)** Representative fluorescent images of ROI plotted over time show the qualitative increase of fluorescent-conjugated BSA concentrations in the tissue surrounding the vessel. **(C)** and **(D)** representative plots of FI normalized to the midvessel intensity for 150-, 350-, and 550-μm vessel distance and 10, 20, and 50 min of perfusion, respectively, demonstrate an increase in tissue-conjugated BSA concentrations as a function of time and distance from the targeted vessel. Protein concentrations at 550 μm distance from the vessel wall reaches saturation at 50 min of perfusion. ($n=4$; mean ± SD). **(E)** Macroscopic picture of catheterized and blood perfused tissue flap. (#, 28G catheter in main coronary artery; *, capillaries; +, erythrocyte accumulation and extravasation in capillaries). **(F, G)** Microscopic images before and after blood perfusion, showing the patent and integer vessel system with blood filled capillaries (*, capillaries). (See also Supplementary Movie SM2). Color images available online at www.liebertpub.com/tec

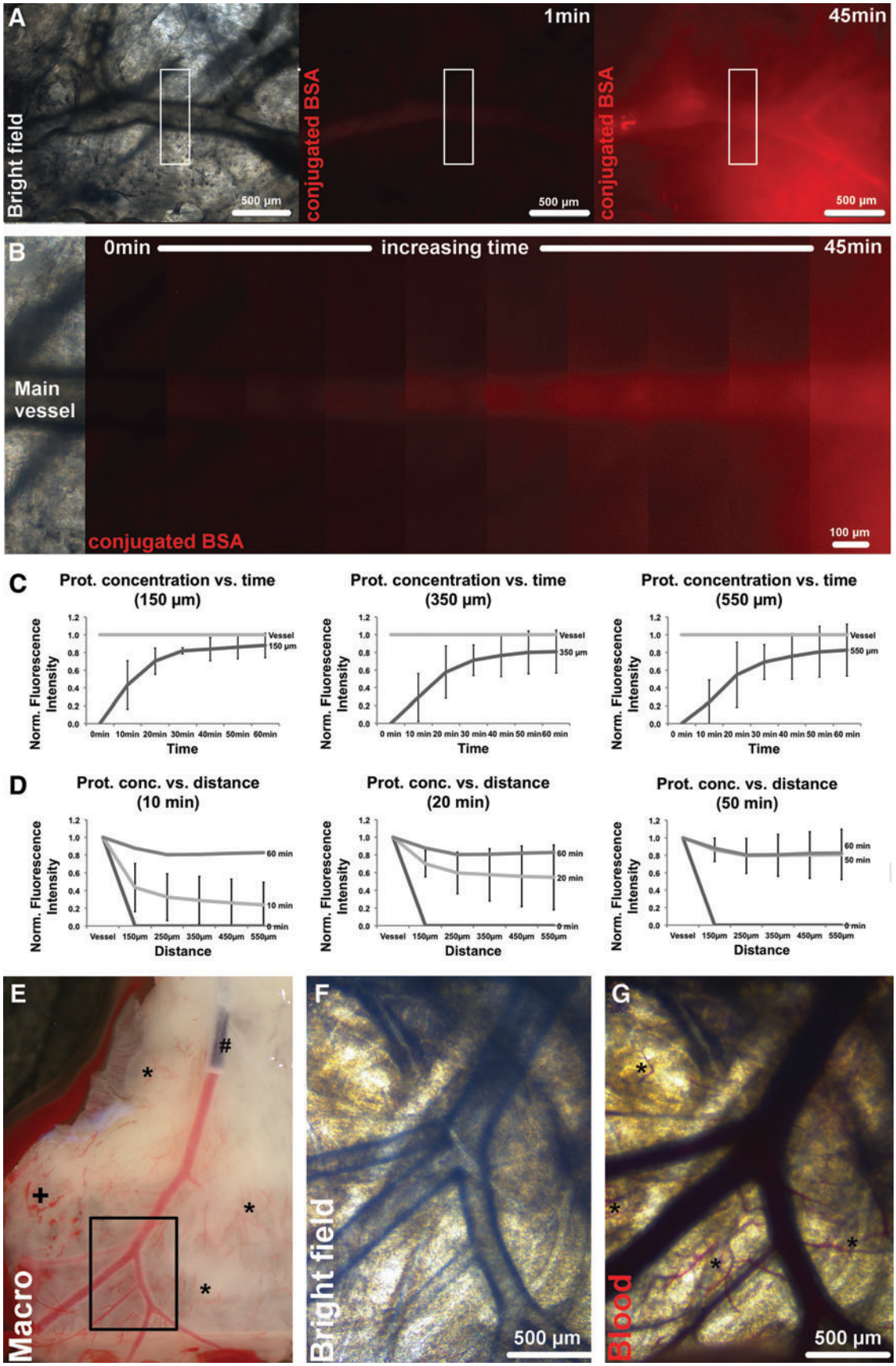
A
Bright field
500 µm
1min
conjugated BSA
500 µm
45min
conjugated BSA
500 µm
B
0min
increasing time
45min
Main vessel
conjugated BSA
100 µm
C
Prot. concentration vs. time (150 µm)
Norm. Fluorescence Intensity
Vessel
150 µm
0min 10min 20min 30min 40min 50min 60min
Time
Prot. concentration vs. time (350 µm)
Vessel
350 µm
0 min 10 min 20 min 30 min 40 min 50 min 60 min
Time
Prot. concentration vs. time (550 µm)
Vessel
550 µm
0 min 10 min 20 min 30 min 40 min 50 min 60 min
Time
D
Prot. conc. vs. distance (10 min)
60 min
10 min
0 min
Vessel 150µm 250µm 350µm 450µm 550µm
Distance
Prot. conc. vs. distance (20 min)
60 min
20 min
0 min
Vessel 150µm 250µm 350µm 450µm 550µm
Distance
Prot. conc. vs. distance (50 min)
60 min
50 min
0 min
Vessel 150µm 250µm 350µm 450µm 550µm
Distance
E
Macro
F
Bright field
500 µm
G
Blood
500 µm

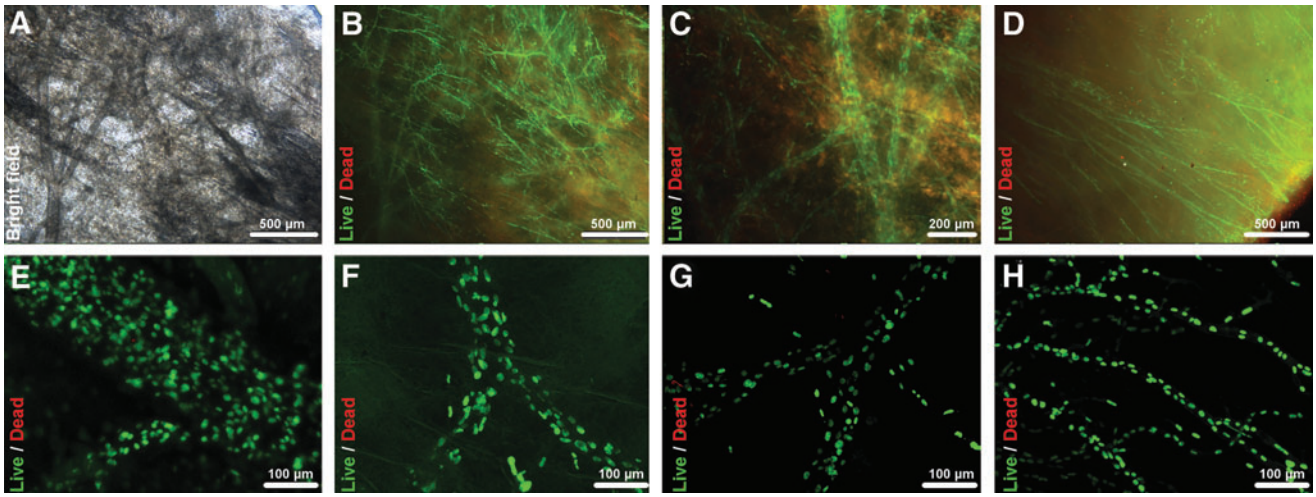

FIG. 4. Selective coronary artery repopularization of the coronary artery tissue-flap model I. Live/Dead assay of coronary perfusion cell-seeded coronary artery tissue flaps (3T3, 5×10^5 cells mL^{-1}) showed highly vital cells lining the complete coronary artery vessel system from the epicardial branches of up to ca. 250-µm vessel diameter down to the capillary system and reaching the edge of the tissue flaps. **(A–D)** Representative bright field and fluorescent images of repopulated main and capillary vessels stained by live/dead staining of the cell bodies via calcein-AM and ethidiumhomodimer showing highly vital cells inside the vessel perimeters. **(D)** Bottom right corner showing repopulated vessels reaching the edge of the tissue flap. **(E–H)** Representative confocal microscope z-stack overlays (z = 60–120 µm) of repopulated main and single-cell capillary-like vessels stained by live/dead staining of the cell nuclei via SYBR-Green and PI showing highly vital cells inside the 3D vessel perimeters. Vital cells, green; nonvital cells, red. Color images available online at www.liebertpub.com/tec

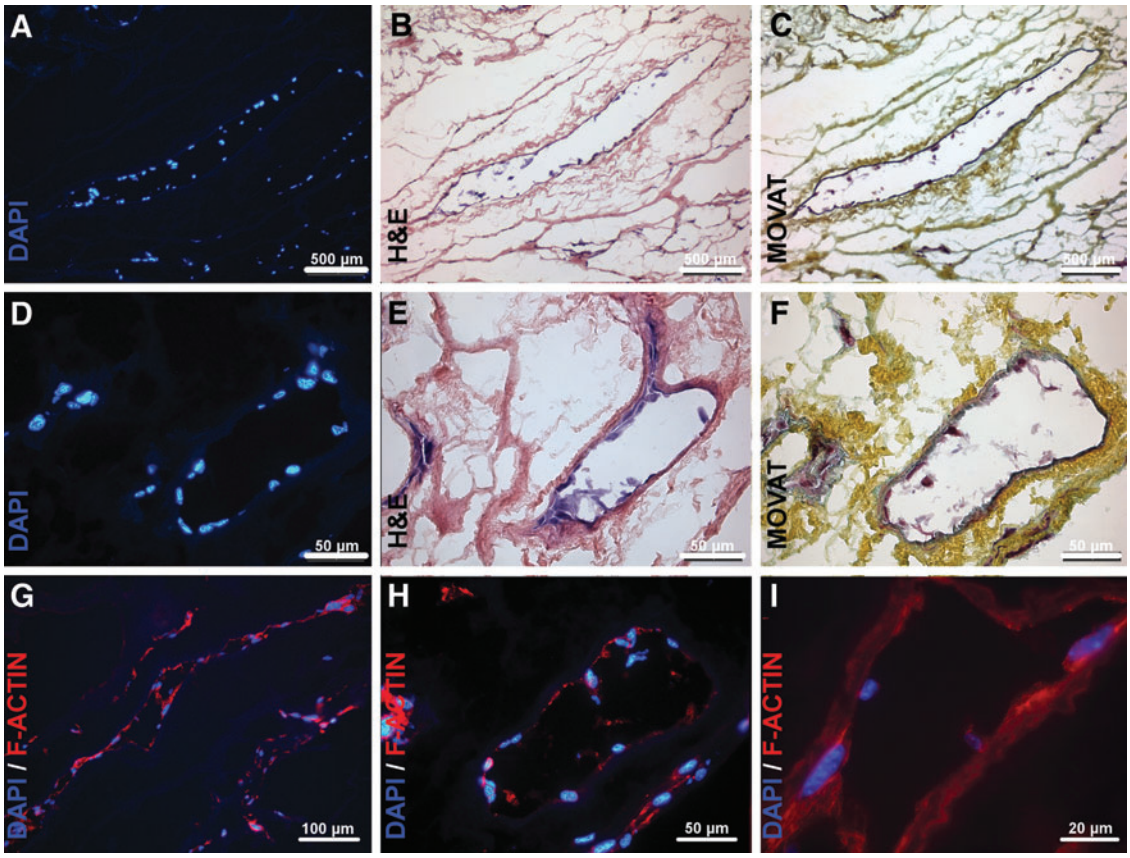

FIG. 5. Selective coronary artery repopularization of the coronary artery tissue-flap model II. Histological analysis of coronary perfusion cell-seeded coronary artery tissue flaps (3T3, 5×10^5 cells mL^{-1}) showed repopularization to be highly selective to the coronary artery vessel system, with apparent cell adherence to the vessel ECM and without cell migration into the adjacent myocardial tissue. Cytoskeleton staining via F-actin staining revealed vessel lumina not only to remain patent despite cell repopularization, but also to be populated with a thin cell layer confluently coating the luminal vessel side of the coronary artery system. **(A–F)** Representative images of repopulated coronary vessels via DAPI, H&E, and Movat staining, respectively. **(G–I)** Representative images of repopulated coronary vessels. Blue, cell nuclei (DAPI); red, cytoskeleton (F-actin). Color images available online at www.liebertpub.com/tec

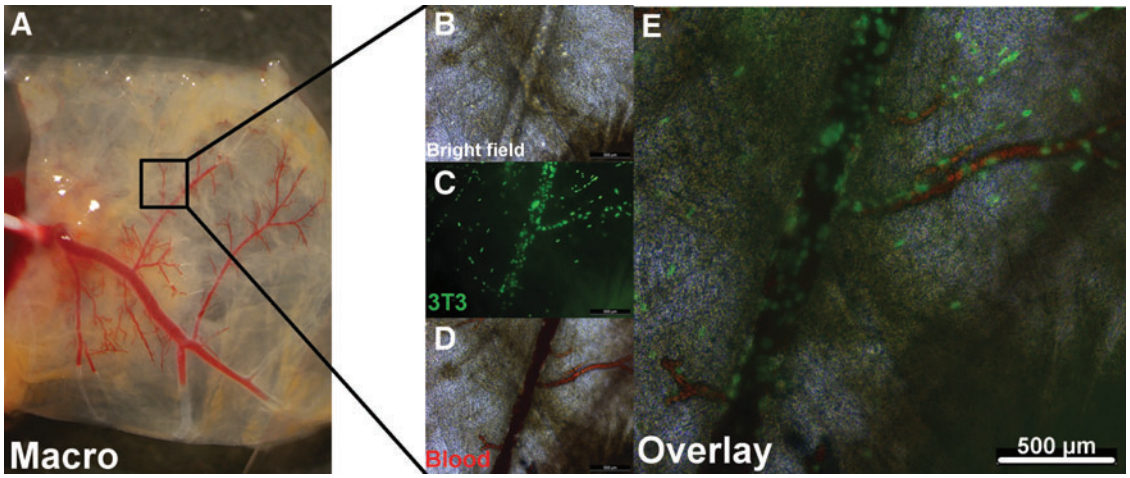

FIG. 6. Blood perfusion of the repopulated coronary artery tissue flap I. Citrated whole blood was manually perfused through the repopulated coronary artery vessel system (3T3, 5×10^5 cells mL^{-1}) via selective coronary ostium catheterization. Macroscopic and microscopic analysis showed patency and proper sealing of the repopulated vessel system for cellular whole blood components for main vessels as well as single-cell repopulated capillary-like structures. **(A)** Representative macroscopic image of blood perfused repopulated tissue flap at the beginning of perfusion. **(B, D)** Representative bright field microscopic image of repopulated vessel before and during blood perfusion. **(C)** Fluorescence microscopic image of the same vessel showing repopulation with vital cells. Cell nuclei stained with SYBR-Green; green, vital cells. **(E)** Overlay of **(C, D)**. (See also Supplementary Movie SM3). Color images available online at www.liebertpub.com/tec

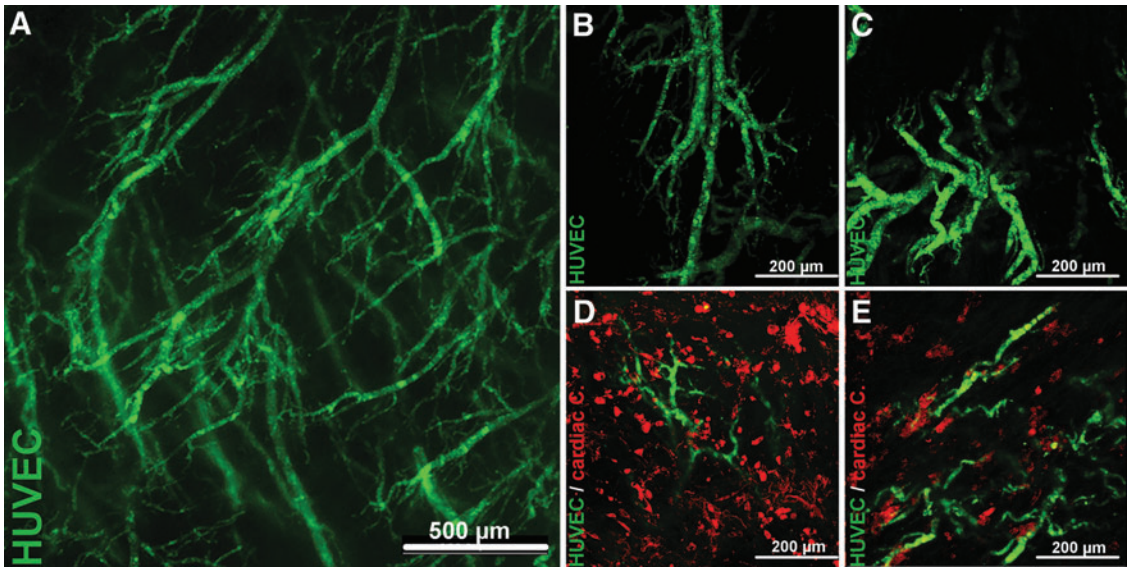

FIG. 7. Live cell tracking and controlled coculture of the coronary artery tissue-flap model I. Endothelial cells (HUVECs) were labeled with green fluorescent CMFDA and used for re-endothelialization of the coronary artery tissue flaps through coronary perfusion of the *in toto* decellularized hearts (5×10^5 cells mL^{-1}). Live fluorescent imaging of the myocardial tissue 24 h after seeding showed extensive and vital endothelial, vascular-like networks inside the vessel system of the decellularized scaffolds. Subsequent surface seeding of the re-endothelialized coronary artery tissue flaps with red fluorescent CMPTX-labeled primary cardiac cells isolated from neonatal rat hearts (2×10^5 cells mL^{-1}) led to cardiac cells in direct juxtaposition to endothelial structures, indicating a controlled coculture of both cell types. **(A)** Representative overview of endothelial networks inside the coronary vessel system of the decellularized myocardial tissue. **(B, C)** Representative confocal microscope z-stack overlays ($z=60$–$100\,\mu m$) of vascular-like structures formed by endothelial cells inside the vessel perimeters. **(E, D)** Representative confocal microscope z-stack overlays ($z=60$–$100\,\mu m$) after additional coculture of re-endothelialized tissue flaps with primary isolated cardiac cells. Green, cytoskeleton of CMFDA-labeled HUVEC; red, cytoskeleton of CMPTX-labeled primary isolated cardiac cells. Color images available online at www.liebertpub.com/tec

biologically derived model offers a predesigned vessel tree architecture with a preserved circumjacent ECM, therefore mimicking nature's input to the highest possible degree. The advantage of such a model to purely cell-based models or synthetic scaffold models lies in the biologically predefined vessel tree geometry, including an optimal 3D spatial distribution of main and capillary vessels that is critically relevant for functional oxygen and nutrient supply as well as carbon dioxide and waste removal.[13] The production out of *in toto* decellularized hearts, which can be generated in high volume through standardized automated software-controlled coronary perfusion with well-studied and reproducible ECM characteristics[10] further guarantees a high degree of standardization and reproducibility despite being a biologically derived model.

In the initial evaluation of the presented coronary artery tissue-flap model, we were able to show the patency and integrity of the de-endothelialized coronary artery vessel system as well as its potential for highly selective vessel repopularization. Coronary artery vessel system repopularization was not only achieved with nonendothelial donor cells, but also with primary HUVECs, resulting in consistent and extensive colonization of the coronary artery system with endothelial networks, filling the vessel perimeters of the tissue flaps with complex vascular structures, while retaining vessel for blood perfusion. Additional coculture with primary cardiac cells led to potentially contractile cells in direct juxtaposition to vascular structures formed by ECs inside the vessel system, although it should be noted that coculture seeding modalities and culture conditions still need to be improved in the future. In addition, functionality of endothelial and cardiac cells in the repopulated tissue flaps still need to be analyzed, including the evaluation of cell-to-ECM and cell-to-cell contacts, which was out of the scope of this initial study. Nonetheless, the results of this study highlight the high potential for re-endothelialization of the decellularized coronary artery vessel system, in terms of a functional 3D vascularization of the coronary artery tissue flaps.

In analogy to the presented model, other biologically derived vascularization models originating from different native tissues[14–16] have already been able to show that re-endothelialization of de-endothelialized vessels altogether with differentiation and proliferation of donor ECs is not only possible, but can also be promoted using different proangiogenic factors, such as CCN1.[17] However, in comparison with other biologically derived models, for example, vascularized tissue constructs derived from small intestine mucosa,[14] one limitation of the presented model lies in the lack of an intact venous drainage system. For though perfusate drainage is assured at the edges of the tissue flaps so that physiological flow conditions could theoretically be simulated *in vitro*, there remains no downstream draining system in the sense that the whole model could be functionally anastomosed to a circulating blood flow *in vivo*, as has been previously shown to promote *in vivo* endothelialization.[18] Nonetheless, the strength of the presented model lies in the possibility to study re-endothelialization and endothelial function of different donor cell types and interactions with cocultured cardiac cells in a simple, but highly standardized 3D *in vitro* model directly derived from native cardiac tissue. Additionally, the model as a whole not only allows controlled perfusion of the vascular tree through selective coronary artery catheterization, but the dimensions and characteristics of the acellular tissue flaps allow for live cell tracking and imaging, which is more difficult to achieve in other models of more dense scaffold characteristics.[19]

The coronary vascular system of the heart, from which the presented model is directly derived, has showed to be an integrated system of particular complexity, in which, coronary vessels and cardiac endothelia play a critical role in heart physiology and pathophysiology.[6, 7] Although major efforts in current cardiovascular research concentrate in replicating and downscaling cardiac biology *in vitro* for the creation of real-tissue-like test systems for pharmaceutical drug and stem cell differentiation studies,[20] recapitulating cardiac tissue, including vascularization still remains a major challenge. Multiple downscaled *in vitro* models have managed to create contractile 3D constructs in simplified biological systems in the past.[21] However, models solely focusing on contractile cardiac constructs and omitting the cardiac vascular system lack biological fidelity, which is important though, for the *in vivo* translation of *ex vivo* tested cardiac models.

In contrast to such models, the here presented *native derived* coronary artery tissue-flap model is directly derived from native cardiac tissue mimicking the *in vivo* cardiac extracellular microenvironment to a degree not yet possible to achieve with synthetic materials or other noncardiac-derived biological models.[2] A key feature is the well-defined coronary vessel architecture and geometry with the LCA and RCA vessel tree embedded in the native ECM of the respective left and right ventricle with high cytocompatibility of the tissue, as shown in this study, offering the possibility to study and recreate coronary vascular biology with high biological fidelity. However, further studies evaluating which EC populations and which additional modalities to promote and enhance EC differentiation, proliferation, and function will be most suitable for functional tissue vascularization are needed and were out of the main scope of this initial pilot study.

Conclusions

Although tissue-engineering approaches have led to significant progress in the quest of finding a viable substitute for the dysfunctional myocardium in the past, the vascularization of such bioartificial constructs still remains a major challenge. The here presented coronary artery tissue-flap model provides a platform for studying re-endothelialization and endothelial function of different donor cell types and their interaction with cardiac cells in a standardized, high-volume producible, low-cost, and reasonably downscaled vascularized cardiac *in vitro* model with high biological fidelity. This might offer the possibility to test and evaluate vascularization strategies as well as to create real-cardiac-like test systems for *in vitro* drug testing and stem cell differentiation studies.

Acknowledgments

We kindly thank Prof. Dr. Gesine Kögler from the Institute for Transplantation Diagnostics and Cell Therapeutics of the Heinrich-Heine-University Düsseldorf for providing the HUVECs and for the fruitful discussions and valuable comments throughout the progress of the project. Further,

we would like to express special gratitude to Mrs. Susanne Bunnenberg for her generous donation that made this project possible in the first place.

Disclosure Statement

No competing financial interests exist.

References

1. WHO, World Heart Federation, World Stroke Organization. Global Atlas on cardiovascular disease prevention and control. WHO, Geneva, Switzerland, 2011.
2. Vunjak-Novakovic, G., Lui, K.O., Tandon, N., and Chien, K.R. Bioengineering heart muscle: a paradigm for regenerative medicine. Annu Rev Biomed Eng **13,** 245, 2011.
3. Novosel, E.C., Kleinhans, C., and Kluger, P.J. Vascularization is the key challenge in tissue engineering. Adv Drug Deliv Rev **63,** 300, 2011.
4. Jain, R.K., Au, P., Tam, J., Duda, D.G., and Fukumura, D. Engineering vascularized tissue. Nat Biotechnol **23,** 821, 2005.
5. Carmeliet, P., and Jain, R.K. Angiogenesis in cancer and other diseases. Nature **407,** 249, 2000.
6. Aird, W.C. Phenotypic heterogeneity of the endothelium: I. Structure, function, and mechanisms. Circ Res **100,** 158, 2007.
7. Aird, W.C. Phenotypic heterogeneity of the endothelium: II. Representative vascular beds. Circ Res **100,** 174, 2007.
8. Hsieh, P.C., Davis, M.E., Lisowski, L.K., and Lee, R.T. Endothelial-cardiomyocyte interactions in cardiac development and repair. Annu Rev Physiol **68,** 51, 2006.
9. Ott, H.C., Matthiesen, T.S., Goh, S.K., Black, L.D., Kren, S.M., Netoff, T.I., and Taylor, D.A. Perfusion-decellularized matrix: Using nature's platform to engineer a bioartificial heart. Nat Med **14,** 213, 2008.
10. Akhyari, P., Aubin, H., Gwanmesia, P., Barth, M., Hoffmann, S., Huelsmann, J., *et al.* The quest for an optimized protocol for whole-heart decellularization: a comparison of three popular and a novel decellularization technique and their diverse effects on crucial extracellular matrix qualities. Tissue Eng Part C Methods **17,** 915, 2011.
11. Akhyari, P., Kamiya, H., Gwanmesia, P., Aubin, H., Tschierschke, R., Hoffmann, S., *et al. In vivo* functional performance and structural maturation of decellularised allogenic aortic valves in the subcoronary position. Eur J Cardiothorac Surg **38,** 539, 2010.
12. Akhyari, P., Fedak, P.W., Weisel, R.D., Lee, T.Y., Verma, S., Mickle, D.A., *et al.* Mechanical stretch regimen enhances the formation of bioengineered autologous cardiac muscle grafts. Circulation **106(12 Suppl1),** I137, 2002.
13. Kannan, R.Y., Salacinski, H.J., Sales, K., Butler, P., and Seifalian, A.M. The roles of tissue engineering and vascularisation in the development of micro-vascular networks: A review. Biomaterials **26,** 1857, 2005.
14. Mertsching, H., Walles, T., Hofmann, M., Schanz, J., and Knapp, W.H. Engineering of a vascularized scaffold for artificial tissue and organ generation. Biomaterials **26,** 6610, 2005.
15. Uygun, B.E., Soto-Gutierrez, A., Yagi, H., Izamis, M.L., Guzzardi, M.A., Shulman, C., *et al.* Organ reengineering through development of a transplantable recellularized liver graft using decellularized liver matrix. Nat Med **16,** 814, 2010.
16. Petersen, T.H., Calle, E.A., Zhao, L., Lee, E.J., Gui, L., Raredon, M.B., *et al.* Tissue-engineered lungs for *in vivo* implantation. Science **329,** 538, 2010.
17. Bär, A., Dorfman, S.E., Fischer, P., Hilfiker-Kleiner, D., Cebotari, S., Tudorache, I., *et al.* The pro-angiogenic factor CCN1 enhances the re-endothelialization of biological vascularized matrices *in vitro*. Cardiovasc Res **85,** 806, 2010.
18. Mertsching, H., Schanz, J., Steger, V., Schandar, M., Schenk, M., Hansmann, J., *et al.* Generation and transplantation of an autologous vascularized bioartificial human tissue. Transplantation **88,** 203, 2009.
19. Gantenbein-Ritter, B., Sprecher, C.M., Chan, S., Illien-Jünger, S., and Grad, S. Confocal imaging protocols for live/dead staining in three-dimensional carriers. Methods Mol Biol **740,** 127, 2011.
20. Grosberg, A., Alford, P.W., McCain, M.L., and Parker, K.K. Ensembles of engineered cardiac tissues for physiological and pharmacological study: Heart on a chip. Lab Chip **11,** 4165, 2011.
21. Schussler, O., Chachques, J.C., Mesana, T.G., Suuronen, E.J., Lecarpentier, Y., and Ruel, M. 3-dimensional structures to enhance cell therapy and engineer contractile tissue. Asian Cardiovasc Thorac Ann **18,** 188, 2010.

Address correspondence to:
Hug Aubin, MD
Department of Cardiovascular Surgery
Heinrich Heine University Düsseldorf
Moorenstr. 5
Düsseldorf 40225
Germany

E-mail: hug.aubin@med.uni-duesseldorf.de

Received: December 1, 2012
Accepted: April 12, 2013
Online Publication Date: June 4, 2013